Design and Realization of a Planar Near Field Antenna Measurement System

Yavuz Öztürk[1,2]*, Fatih Üstüner*[1]

[1]TÜBITAK BILGEM UEKAE[*], Gebze Yerleşkesi, Kocaeli, Türkiye.
yavuz.ozturk@uekae.tubitak.gov.tr, fatih.ustuner@uekae.tubitak.gov.tr,

[2]Gebze Institute of Technology (GYTE)
Physics Department, Gebze/Kocaeli

Abstract

Determination of the radiation pattern is one of the major issues in antenna characterization. Radiation pattern is a far field parameter and it must be measured at a point where wave trains are propagating in same phase. Although this range can be obtained inside a laboratory for isotropic antennas, in case of high gain directive antennas it can well extend to several tens of meters. Radiation pattern measurement using near field approach is possible for the latter case, even inside a small-scale laboratory. Nevertheless, since the design and the realization of near field antenna measurement systems require detailed engineering activities compared to that of far field systems, their costs are fairly high. In order to obtain a low-cost, maintainable and native near field antenna measurement system, an engineering study was conducted in TUBITAK BILGEM UEKAE EMC Laboratory and a near field measurement system was developed. In this article, antenna patterns measured by the developed system are presented.

1. Introduction

Radiation pattern of an antenna becomes meaningful in the far field range, in the so-called Franhaufer region of the source. That is because wave trains move at same phase in this region, namely propagation direction of the waves become perpendicular to phase direction [1]. For high gain directive antennas this range is unfortunately far beyond the laboratory scales. For instance - starting from the classical equation $2D^2/\lambda$ – a 40 dB gain reflector antenna, 1 meter in diameter, radiating at 10 GHz frequency, will have a far field range about 70 meters. Conventional far field radiation pattern measurement techniques require an open area test site which has adequate dimensions for handling these distances. However, constructing and maintaining such an infrastructure is rather cumbersome. There are several problems one has to deal with performing measurements outside. Especially, unavoidable reflections from land and surroundings pose a big problem on healthful measurements. Additionally, open area tests directly depend on meteorological conditions. Yet, due to weather, climate and daytime considerations, test time is highly restricted. Moreover, environmental elements such as rain, snow, frost, damp etc. will damage the facility itself by the time. This damage will cause loss of time and manpower, along with its financial burden. Working at open area test sites is also problematic for test personnel. Transportation of personnel and equipments are another big issue to determine the test time.

Near field measurements require a sensitive and accurate mechanical infrastructure as well as a mathematical transformation of the near field data to far field. In turn they shorten the distance between antenna under test (AUT) and measuring probe to several times of the wavelength of measurement frequency. In addition to that, due to other advantages such as; reliability, accuracy and repeatability in the measurements, its time saving swiftness, minimization of personnel requirements, elimination of transportation difficulties (from both personnel and equipment aspects), performing of tests without interruption in a closed, safe and secure environment, near field measurement is preferred to far field measurements in open area [2]. Nevertheless since the design and realization of near field measurement systems involves, extra engineering labor compared to far field systems, turn-key systems are rather costly.

For the sake of attaining a low-cost, maintainable and native system, an engineering activity has been pursued in TUBITAK BILGEM UEKAE EMC Laboratory and a planar near field measurement scanner system has been constructed (Figure 1a-1b). The X-Y scanner, which is the mechanical backbone of the system, has been built by using general purpose linear mechanical components. Open-ended rectangular cross-section waveguides are employed as measurement probe, as well as a sensitive rotary actuator rotating the probe to two polarizations has also been installed. Different probes have been designed for different frequency bands using waveguides of different dimensions, considering standard waveguide frequency bands. Since data should be taken in every half wavelength ($\lambda/2$), an automation platform involving motors, control units and computer has been established.

[*]The Scientific and Technological Research Council of Turkey, Center of Research for Advanced Technologies of Informatics and Information Technology

978-1-4244-6051-9/11/$26.00 ©2011 IEEE

Unintended Z plane motion while the scanner is operating has been measured by the National Metrology Institute (TUBITAK UME) by utilizing dimensional metrological equipments. These measurements have shown that, the deviation from Z-plane planarity is within ±500 µm, throughout the full scan area of 1.8 x 4.0 m, which corresponds to a 1.6% phase error at most for 10 GHz.

A vector network analyzer (Agilent E8362B) is employed as the measurement equipment, and it is fed by an external trigger generated by motor drivers for synchronization and for the sake of measurement rapidity. S21 parameter (both magnitude and phase) is measured in every half wavelength of the measurement frequency in X-Y plane for two polarizations. Gathered data is transformed using two dimensional Fourier transforms. In order to consider deviations due to the probe itself, probe compensation is also taken into account (Figure 1c).

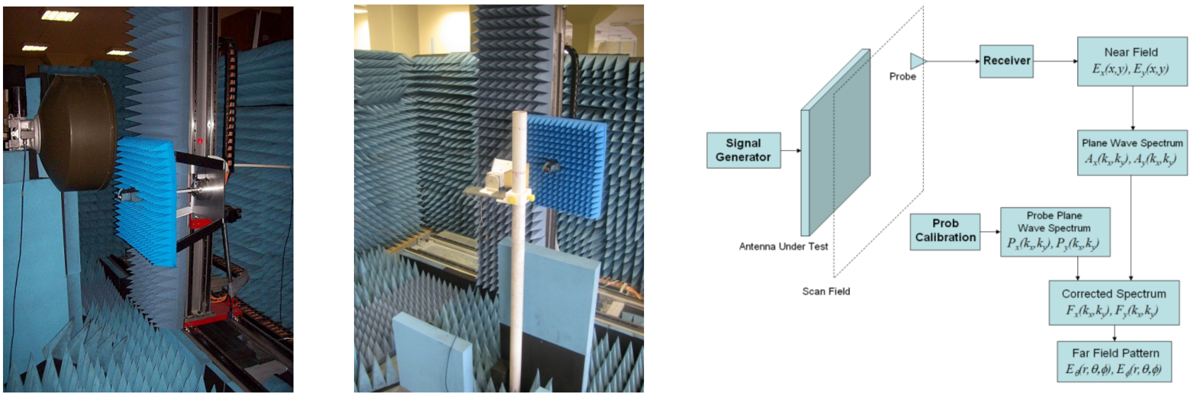

(a) **(b)** **(c)**

Figure 1 (a)(b) Near Field Measurement System, (c) Near Field – Far Field Transformation Algorithm

2. Near Field Measurement Theory

Helmholtz wave equations for source-free, linear, homogeneous, isotropic media can be put down as follows:

$$\nabla^2\mathbf{E} + k^2\mathbf{E} = 0, \quad \nabla^2\mathbf{H} + k^2\mathbf{H} = 0 \tag{1}$$

Here k is the wave number and it is the mode of a vector which shows the propagation direction. Since k is constant k_z component can be eliminated.

$$\mathbf{k} = \mathbf{a}_x k_x + \mathbf{a}_y k_y + \mathbf{a}_z k_z, \qquad \mathbf{k}\cdot\mathbf{k} = k^2 = {k_x}^2 + {k_y}^2 + {k_z}^2 = \left(\frac{2\pi}{\lambda}\right)^2 \tag{2}$$

$$k_z = \begin{cases} \sqrt{k^2 - {k_x}^2 - {k_y}^2} & {k_x}^2 + {k_y}^2 \leq k^2 \\ -j\sqrt{{k_x}^2 + {k_y}^2 - k^2} & {k_x}^2 + {k_y}^2 > k^2 \end{cases} \tag{3}$$

Any monochromatic wave can be defined in terms of same frequency plane waves propagating in different directions having different amplitude: $\mathbf{E} = \frac{1}{4\pi^2}\int_{-\infty}^{\infty}\int_{-\infty}^{\infty}\mathbf{A}(k_x,k_y)e^{-j\mathbf{k}\cdot\mathbf{r}}dk_x dk_y$**.** Starting from here, three components of $\mathbf{E}$ can be written as follows:

$$E_{x,y,z}(x,y,z) = \frac{1}{4\pi^2}\int_{-\infty}^{\infty}\int_{-\infty}^{\infty} A_{x,y,z}(k_x,k_y)e^{-jk_z z}e^{-j(k_x x + k_y y)}dk_x dk_y \tag{4}$$

Only two components of **A(k)** can chosen independently for arbitrary k_x, k_y ve k_z. Thus we can state the above structure for an x-y plane at $z = z_o$ as:

$$E_{x,y}(x,y,z=z_o) = \frac{1}{4\pi^2}\int_{-\infty}^{\infty}\int_{-\infty}^{\infty}\left[A_{x,y}(k_x,k_y)e^{-jk_z z_o}\right]e^{-j(k_x x + k_y y)}\,dk_x\,dk_y \tag{5}$$

These equations are actually two dimensional Fourier transforms. In view of the fact that, for directive antennas electrical field is accumulated around the vicinity of the antenna, we may concretize boundaries for the Fourier transform:

$$A_{x,y}(k_x,k_y) \approx e^{j(k_z d)}\int_{-b/2}^{+b/2}\int_{-a/2}^{+a/2} E_{x,y}(x,y,z=d)e^{\,j(k_x x + k_y y)}\,dx\,dy \tag{6}$$

The purpose of plane wave expansion is to determine the directions and the amplitudes of plane waves in the superposition. Tangent coefficients of the electric field measured on the $z = z_o$ plane give us this opportunity. Amplitude function **A** is known as wave number spectrum of electrical field. Measurement within finite area is only true for directive antennas which have negligible side and back lobes. Here the transition between spatial domain and ($k_x - k_y$ domain) and angular domain ($\theta - \phi$ domain) is done by using $k_x = k\,\sin\theta\cos\phi$,

$k_y = k\ \sin\theta \sin\phi$, $k_z = k\ \cos\theta$ relations. Starting from that, far-field pattern of the antenna in a plane-wave spectrum function is calculated as follows:

$$E_\theta(r,\theta,\phi) \approx j\frac{k\,e^{-jkr}}{2\pi r}(A_x\ \cos\phi + A_y \sin\phi) \quad (7)$$

$$E_\phi(r,\theta,\phi) \approx j\frac{k\,e^{-jkr}}{2\pi r}\cos\theta\,(-A_x\ \sin\phi + A_y \cos\phi) \quad (8)$$

Here $\theta = \sin^{-1}\left[\sqrt{k_x^2 + k_y^2}/k\right]$ and $\phi = \tan^{-1}(k_y/k_x)$ [2,3].

In planar scanning, the probe travels on a plane in front of test antenna and complex signal data is saved considering corresponding spatial position of the probe (Fig 1b). During the scan only x, y motion is allowed, through which large enough area is explored. Antenna must be well aligned in order to obtain desired constant z_o. Antenna-probe (z_o) distance is adjusted to be 3 to 10 times (3λ-10λ) of the measured frequency wavelength. Lower limit is for assuring the probe not to enter into reactive near field region, which may in turn distort the field and exaggerate multiple reflections. The latter limit is for narrowing down the scan area and to get a better signal to noise ratio. Measurement points on the x-y plane builds up a rectangular grid having $\Delta x = \Delta y = \lambda/2$ in order to satisfy Nyquist sampling criteria. Sampling interval smaller than that will not help for a higher resolution in the far field. In order to do so, one has to add extra zeros on the periphery of the gathered data. By that way sampling number is artificially increased so the resolution [3].

Calculating far field pattern requires near field data in both polarizations, vertical and horizontal. However, open-ended rectangular waveguide probe can measure only in one polarization. That is why we installed a sensitive rotary motor which can accurately rotate 90° in order the probe to receive both polarizations. So, every measurement is conducted for both polarizations separately. Scan should cover an area in order that peripheral signals assume at least 45 dB below the maximum signal. Reducing the scan area without disturbing the results will help to save time. Especially in applications in which one doesn't need exact results, such as a radar alignment scan area can be narrowed down to limits above.

Measured complex near field data is converted to plane waves in the k-space by means of the two dimensional Fourier transforms. AUT's plane wave spectrum is distorted because of the angular response of the probe. In order to correct this distortion AUT's planar wave spectrum is proportioned (divided) to probes plane wave spectrum. This treatment is known as probe compensation. Corrected plane wave is further converted to angular domain by using angular transformation equations (Equation 7-8) and far field pattern is obtained.

3. Results

Here we present near field measurement results of our system: for a radiolink antenna (Radiowaves WP2-8NS, SN:15445) at 8 GHz (See Fig 1(a)) and a double-ridged horn antenna (EMCO 3115, SN: 9610-4990) at 10 GHz (See Fig 1(b)). Far field antenna pattern for the radiolink antenna in $k_x - k_y$ domain has been shown in Fig 2. In Fig 3, H-plane and E-plane cross sections of the data in angular domain are compared with their corresponding manufacturer assumed values. It can be seen that, far field results transformed from near field data, fit the radiation pattern envelope anticipated by the manufacturer.

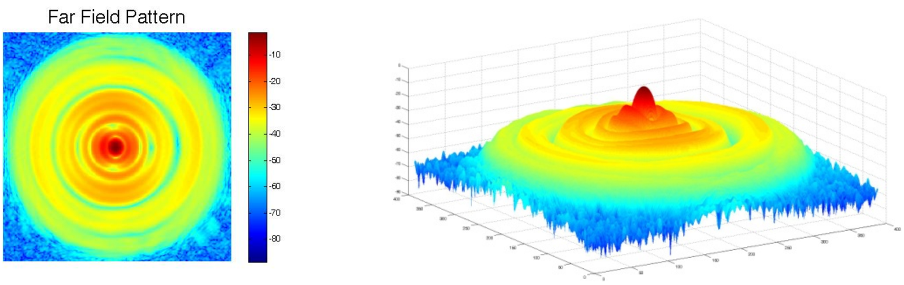

Figure 2, Far Field Pattern for the Radiolink Antenna

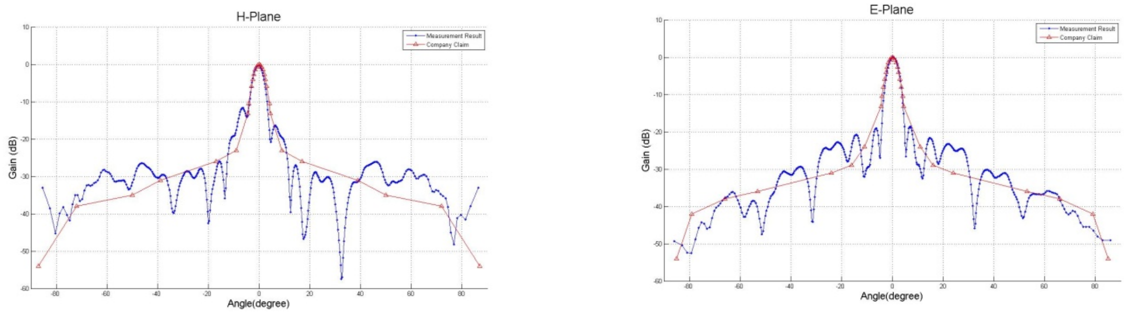

Figure 3, Far field results for radiolink antenna in angular domain compared with their expected values.

Likewise, far field pattern for the double-ridged horn antenna in $k_x - k_y$ domain has been shown in Fig 4. Additionally, 2D antenna pattern specified by the manufacturer for double-ridged horn at 10 GHz is demonstrated to the right most of that figure. Fig 5 is dedicated to H-plane and E-plane cross section comparisons with the manufacturer assumptions. There is again a good agreement, except for the E-plane case where side lobes are exaggerated. That is because double-ridged horn is not highly directed in y-polarization direction and a wider scan is needed in that axis.

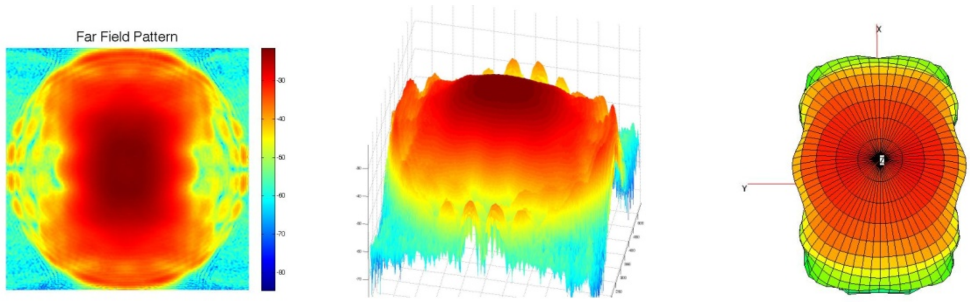

Figure 4, Far Field Pattern for the Double-Ridged Horn Antenna.

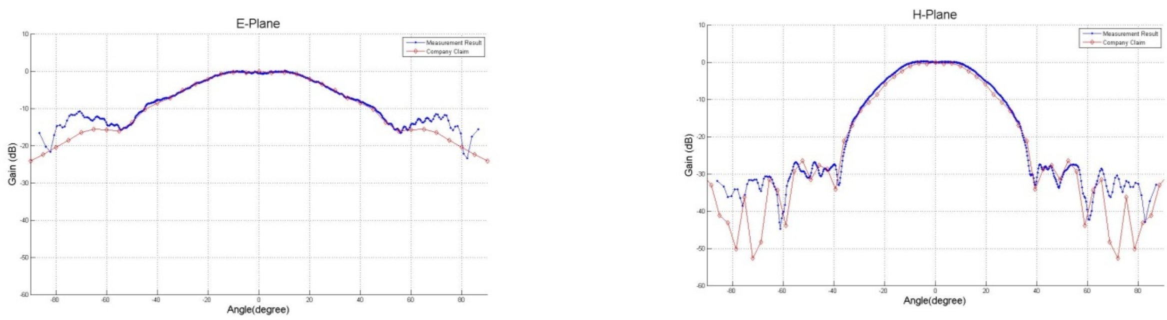

Figure 5, Far field results for double-ridged horn in angular domain compared with their expected values.

4. Conclusion

For the sake of obtaining a low-cost, maintainable near field system, an engineering activity has been pursued in TÜBITAK BILGEM UEKAE EMC Laboratory and a 4.0 m x 1.8 m near field antenna measurement system is developed. The system is basically composed of a sensitive mechanical infrastructure, a vector network analyzer and an automation and signal processing software. Since the system is developed by using common industrial linear mechanical elements and by putting the theory directly into practice cost is reduced to one fifth of equivalent commercial systems.

5. References

[1]. Y. Rahmat-Samii, L.I. Williams ve R.G. Yoccarino, "The UCLA Bi-polar Planar-Near-Field Antenna Measurement and Diagnostics Range", IEEE Antennas & Propagation Magazine, Vol. 37, No. 6, December 1995.

[2]. Yaghjian, A.D.: "An Overview of Near-Field Antenna Measurements", IEEE Transactions on Antenna and Propagation Vol. AP-34, January, 1986.

[3] S. Gregson, J. McCormick ve C. Parini, "Principles of Planar Near-Field Antenna Measurements", IET Electromagnetic Waves Series 53.